Measurement of (p,p) elastic differential cross sections for 17O in the 0.6–2 MeV range at 165°

M. Salimi, O. Kakuee, S F Masoudi, H. Rafi-Kheiri, E. Briand, J.-J. Ganem, Ian Vickridge

Nuclear Instruments and Methods in Physics Research B 516 (2022) 15–22

Contents lists available at ScienceDirect

Nuclear Inst. and Methods in Physics Research, B

journal homepage: www.elsevier.com/locate/nimb

Measurement of (p,p) elastic differential cross sections for ^{17}O in the 0.6–2 MeV range at 165°

M. Salimi [a,b], O. Kakuee [c], S.F. Masoudi [a,*], H. Rafi-kheiri [c], E. Briand [b], J.-J. Ganem [b], I. Vickridge [b]

[a] Department of Physics, K.N. Toosi University of Technology, P.O. Box 15875-4416, Tehran, Iran
[b] Sorbonne Université, CNRS, Institut des NanoSciences de Paris, INSP, SAFIR, F-75005 Paris, France
[c] Physics and Accelerators Research School, NSTRI, P.O. Box 14395-836, Tehran, Iran

ARTICLE INFO

Keywords:
Proton elastic scattering cross section
17O(p,p)17O
Ion beam analysis
EBS
Non-Rutherford Cross section

ABSTRACT

$^{17}O(p,p)^{17}O$ elastic scattering cross sections were measured for the first time, on the INSP SAFIR platform in Paris, using thin silica films prepared by thermal oxidation of Si under $^{17}O_2$. The ^{17}O content of the film was determined by a combination of ellipsometry and IBA measurements.

The yield of elastically scattered protons was determined from the corresponding peak in the Elastic Backscattering spectra, with the underlying Si signal reduced by channeling of the incident beam in the silicon substrate. The measured $^{17}O(p,p)^{17}O$ cross section was determined with a systematic uncertainty of about 14%. The cross section consists of resonant structures superimposed on a smoothly varying component that increases from about 1.2 times the Rutherford cross section at 600 keV to about 3 times Rutherford at 2 MeV. A resonance at 1230 keV shows promise for proton Elastic Backscattering depth profiling, especially at large backscattering angles. The cross section is available on IBANDL (www-nds.iaea.org/ibandl/).

1. Introduction

Proton elastic backscattering spectrometry (EBS) is a powerful method which has been widely used for accurate analysis of materials, such as impurity distributions in thin layers, determination of stoichiometry and elemental areal density. Compared to alpha particle EBS, proton EBS offers useful excursions from the Rutherford cross section, such as enhancements and resonant structures, at lower beam energy than for alpha particle EBS, whilst allowing a similar analysis depth [1-3]. Non-Rutherford proton EBS may thus be used on accelerators with lower energies than those required for EBS with alpha particles. For example, the $^{16}O(\alpha,\alpha)$ and $^{18}O(\alpha,\alpha)$ elastic scattering cross sections are Rutherford below 2 MeV. Although that for ^{17}O has not been measured, it too is highly likely to be Rutherford below 2 MeV. The lower Coulomb repulsion between incident protons and the target nucleus means that the nuclear potential influences the elastic scattering cross section at lower energies than those for alpha elastic scattering, such as that of the well-known narrow resonance at 3.042 MeV in $^{16}O(\alpha,\alpha)^{16}O$ [4,5].

The $^{16}O(p,p)$ EBS cross section is usefully greater than Rutherford between 1 MeV and 2 MeV (Fig. 1) but it is slowly varying and there is no useful resonant structure below 2 MeV [4,5]. As seen in Fig. 2 $^{18}O(p,p)$ has a useful narrow resonance at about 1750 keV. Low energy narrow resonances such as $^{18}O(p,\alpha)$ at 151 keV [6,7] in reactions with high Q-values have been used for concentration depth profiling of ^{18}O so that there has been no push to apply the EBS resonance. The $^{17}O(p,\alpha)$ reaction has a number of narrow resonances, however the low Q-value of 1197 keV means that it is not possible to choose an appropriate thickness for a foil in front of the detector that will allow detection of the alpha particles, but stop the large flux of elastically scattered protons from entering the detector. The higher EBS cross section and simplified equipment needs (no need for high precision beam energy scanning or specialized large area detectors) could make ^{18}O EBS attractive for wider application to stable isotopic tracing, and in this vein, we have also considered ^{17}O EBS. Whilst ^{16}O and ^{18}O have nuclear spin of zero, we note that ^{17}O has a nuclear spin of ½, and can also be used in electron paramagnetic tracing experiments where the spin–orbit coupling renders the response of the ^{17}O nucleus sensitive to its nearest neighbor configuration.

Although we could find no published measurements of $^{17}O(p,p)$ cross sections, extensive measurements of yield curves have been made using

* Corresponding author.
E-mail address: masoudi@kntu.ac.ir (S.F. Masoudi).

https://doi.org/10.1016/j.nimb.2022.01.002
Received 23 September 2021; Received in revised form 20 November 2021; Accepted 4 January 2022
Available online 14 February 2022

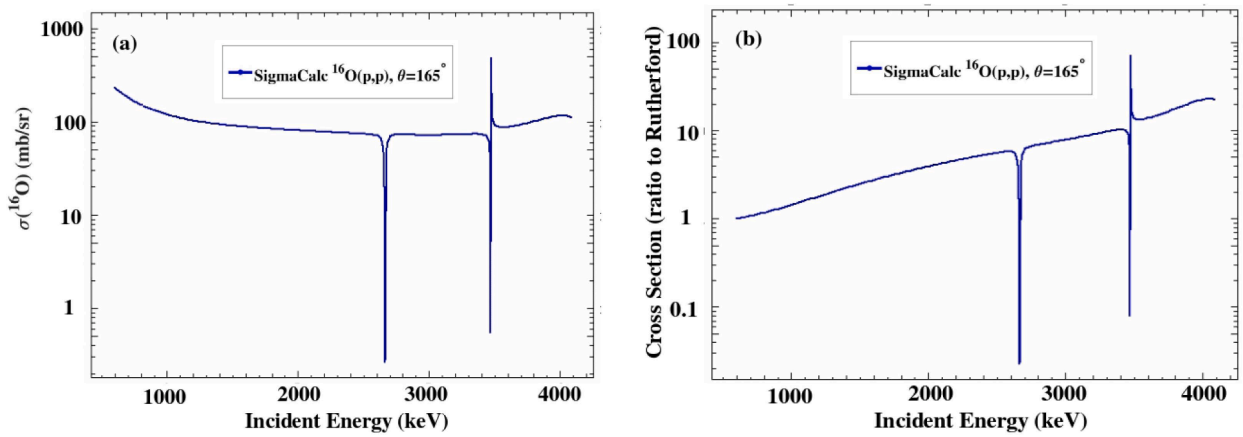

Fig. 1. a) cross section and b) the ratio to the Rutherford cross section of ^{16}O(p,p)^{16}O at 165 (sigmacalc) [4].

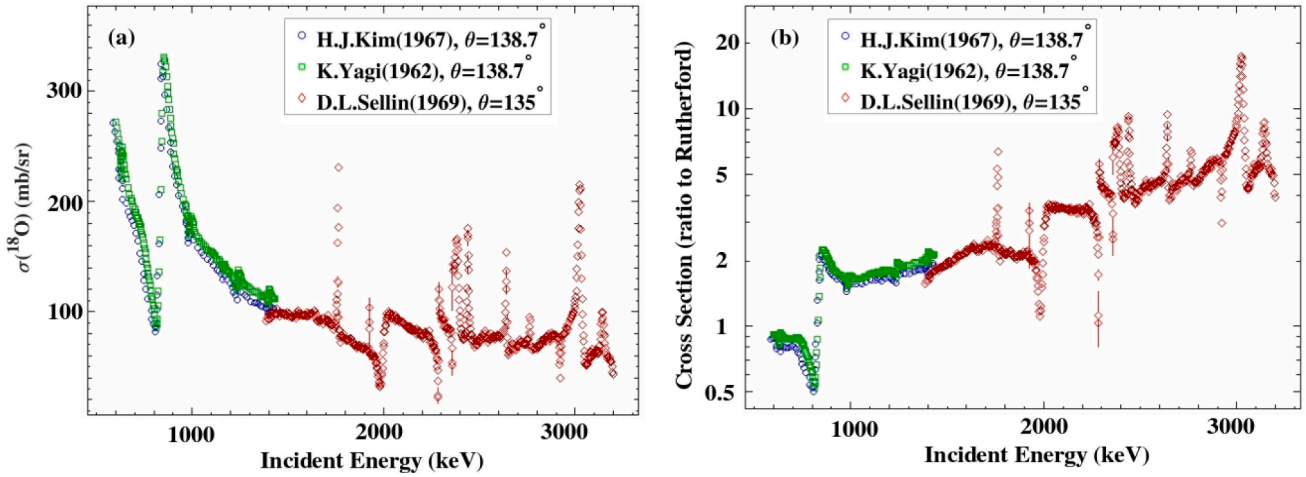

Fig. 2. a) The differential cross section of ^{18}O(p,p)^{18}O near 135° and b) its ratio to Rutherford [10–12].

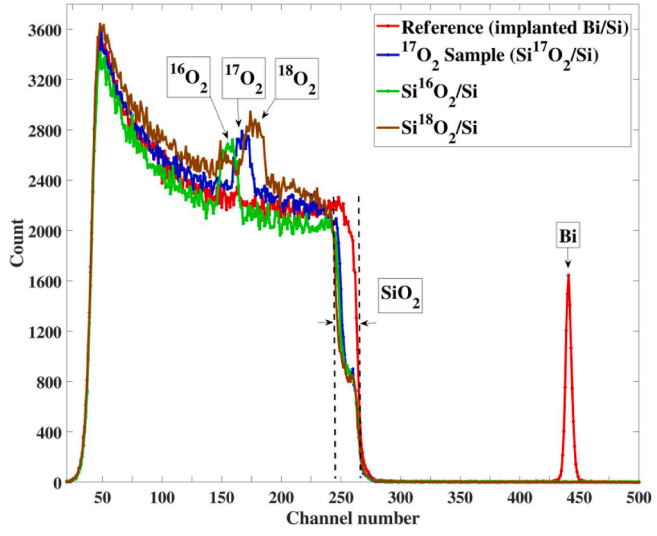

Fig. 3. The typical measured RBS spectra of the three isotopically enriched oxide targets and the Bi reference at scattering angle 165° and E_α = 1.8 MeV.

thin self-supporting SiO or gas targets [8,9]. These measurements, aimed at nuclear physics studies, were concerned with the energies and widths of ^{18}F nuclear levels and so absolute cross sections were not required. In addition, for a significant part of the incident proton energy range of interest here, of 600 to 2000 keV [8] the authors of the work were only able to use oxygen gas enriched to 76.6% in ^{17}O, with contamination of 18.2% in ^{18}O and 5.2% in ^{16}O. Properly correcting the measured yields (the three isotopes are probably not resolved in the charged particle energy spectra) would require absolute measurements of the ^{17}O(p,p) cross section and knowledge of the ^{18}O(p,p) and ^{16}O(p,p) cross sections at the angles and energies where the ^{17}O(p,p) yields were measured. The authors therefore simply subtracted 23% of the counts from the non-resonant amplitude. This procedure is probably valid for extracting the level parameters in energy regions where the ^{18}O(p,p) and ^{16}O(p,p) cross sections are varying slowly, but does not guarantee that the measured shape of the yield curve from this gas target is the same as the shape of the cross section. Yield curves were also measured [9] for incident particles in the energy range of 1.4 MeV to 3 MeV, using a thin self-supporting target. The backscattered protons from the three oxygen isotopes could be resolved, at least at backward angles and for the higher incident beam energies, however this energy range does not include a major region of interest here, for the exploitation of low energy proton EBS. We therefore measured the ^{17}O(p,p) cross section in the range from 600 keV to 2 MeV at 165°, the most widely used RBS scattering angle. We will show that the yield curves from Ref. [8] are significantly distorted by the contribution from ^{18}O(p,p) and thus, unfortunately, cannot be simply re-scaled to be used as cross sections for accurate IBA. We will also show discrepancies between our measurements and those of Ref. [9].

2. Experimental methods

Our experimental work was carried out in the channeling chamber on the 30° right beamline of the 2.5 MV Van de Graaff SAFIR (Système d'Analyse par Faisceaux d'Ions Rapides) platform at INSP (Institut des NanoSciences de Paris). During the measurements, the chamber pressure was about 1×10^{-6} mbar. A 300 μm thick, 300 mm^2 surface barrier detector at scattering angle of 150 was used for NRA, and a 100 μm thick, 25 mm^2 surface barrier detector at scattering angle of 165, collimated to exclude edge effects, was used for RBS and EBS measurements. Pulses from the CAEN A1422 preamplifier were treated in a digital data acquisition system based on a CAEN DT5725 digital pulse processor to provide particle energy spectra.

2.1. Energy calibration of the accelerator

The accelerator energy calibration procedure, based on energies of narrow (p,γ) resonances and the signal from the generating voltmeter, is described in Ref. [13].

2.2. Measurement of the detector solid angle-charge product

The detector solid angle-charge product was first determined by RBS, using a standard Bi-implanted Si reference (Ref Bi = 5.64×10^{15} at/cm^2) with an uncertainty of 2%–3%. RBS measurements were performed with a 30nA, 1.8 MeV alpha particle beam of 0.5 mm, and detection at 165°. Total deadtime was less than 10% and was corrected for. The entire vacuum chamber is insulated from ground and is used as a Faraday cup for charge integration, with reproducibility better than 1%. The vacuum of the reaction chamber was about 10^{-6} mbar and the integrated beam charge for each measurement was 10μc.

The parameter $\Omega \times Q$ was defined by RBS as follows:

$$\Omega \times Q = \frac{Y_{Bi}}{N_{Bi}\sigma_{Bi}} \quad (1)$$

where Q, Ω, Y_{Bi}, N_{Bi} and σ_{Bi} represent the charge, the solid angle, the experimental yield of Bi (net area under the Bi peak), and the Rutherford cross section of Bi. $\Omega \times Q$ as defined here will be used in the following experimental work.

2.3. Target preparation

Ideally, gas targets [8], or thin self-supporting targets such as those prepared by anodic oxidation by Amsel for the extensive early ^{16}O and ^{18}O nuclear reaction cross section measurements [14], should be used for these measurements, however we have neither a supply of water highly enriched in ^{17}O for anodic oxidation, nor a gas target chamber and detection system. Although it has been shown to be possible to fabricate thin self-supporting targets [9], our attempts (e.g. by oxidising Al [13]) were also unsuccessful, and so we used thermal silica layers of thicknesses near 100 nm, grown on [1 0 0] oriented silicon wafers by thermal oxidation at 1100 °C in dry $^{17}O_2$ gas in a quartz tube vacuum furnace with a base pressure of 10^{-6} mbar. The choice of silicon substrate has the advantage that the oxidation methods and thermal oxide characteristics are very well known [15]. The disadvantage of this target is that the protons are elastically backscattered from oxygen atoms in the thin oxide surface layer with a lower energy than those backscattered from the silicon, and so the corresponding ^{17}O peak in the spectrum sits on a large and non-Rutherford background of protons scattered from Si, as may be seen in Fig. 3. This complicates peak area extraction. Thermal ^{17}O oxides could conceivably be made on heavier substrates where the substrate signal would at least be Rutherford, but of course in this case the substrate signal amplitude would swamp the ^{17}O elastic scattering signal.

We also made samples in $^{16}O_2$ and $^{18}O_2$ gas under the same conditions. RBS spectra from samples highly enriched in each of the stable isotopes, together with a spectrum from the Bi reference, are shown in Fig. 3. The signals from the three oxygen isotopes can be clearly identified, but the overlap of the signals means that RBS is not particularly well suited to determining small quantities of the adjacent masses in the wings of a major component. In our case, this is true for the determination of small quantities of ^{16}O and ^{18}O in the presence of a large majority of ^{17}O. Nevertheless, the spectra are very sensitive to the overall silica thickness, through the energy at which the silicon signal increases from that in the silica layer to that of the silicon substrate.

2.4. Characterization of the thin target

2.4.1. Measurement of the total amount of O by ellipsometry

The thermal oxide of silicon, grown at 1100 °C in pure oxygen, is expected to be very close to stoichiometric [15]. We measured the physical silica thickness and refractive index by ellipsometry. The refractive index at 633 nm varied slightly between 1.47 and 1.48, very close to the refractive index of stoichiometric fused silica which is 1.46 [16]. This provides strong support of the affirmation that this thermal oxide is indeed stoichiometric SiO_2. The density of the thermally grown silica on silicon is taken to be 2.21 g/cm^3 [17]. The small variations in refractive index probably indicate small variations of density, however these would be less than 1% [16], and so an uncertainty of 1% is ascribed to the silica film density, which is used to calculate the total oxygen atomic areal density, assuming stoichiometric SiO_2. Film physical thickness was determined with about 1% uncertainty.

2.4.2. Measurement of the areal density of ^{18}O

The areal density of ^{18}O [$N_{^{18}O}$] was determined by NRA with the $^{18}O(p,\alpha)^{15}N$ reaction [12], which has a high Q-value of 3.97 MeV, providing an isolated peak. The peak of the cross section near 830 keV was used to provide high yields. The beam lost only about 5 keV in the targets and so the cross section hardly varied across the thickness of these samples. A 10 μm mylar film was used in front of the 300-μm-thick surface barrier detector, placed at detection angle of 150, to stop the high flux of protons scattered from the silicon. Absolute values of the areal density [$N_{^{18}O}$] were determined by comparing yields with a standard thermal $Si^{18}O_2/Si$ (Ref $^{18}O = 380 \times 10^{15}$ at/cm^2), with an uncertainty of 2%–3%. Typical spectra are shown in Fig. 4.

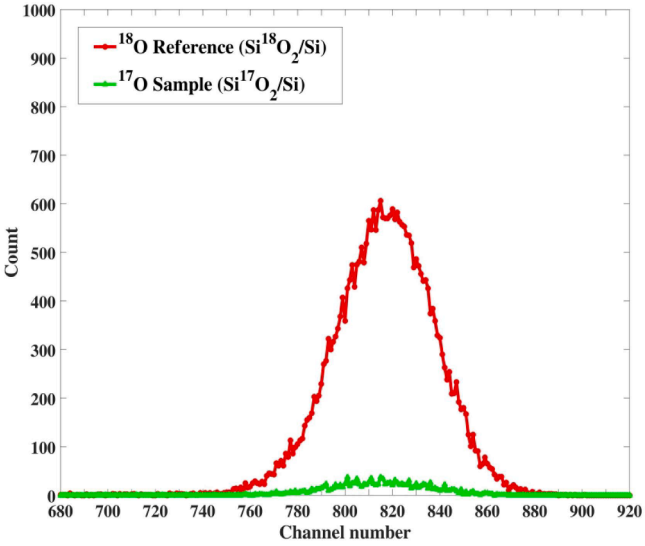

Fig. 4. The typical measured p-NRA spectra obtained from the ^{17}O enriched silica layer used for the cross section measurements, and a reference thin silica layer of natural isotopic composition at scattering angle 150° and Ep = 830 keV.

2.4.3. Measurement of the areal density of ^{16}O

The areal density of ^{16}O [N_{16O}] was determined by NRA with the ^{16}O (d, p_1)^{17}O reaction [1,18] with a deuteron beam of 860 keV. The protons from the reaction were detected with a 300 μm thick surface barrier detector placed at 150 scattering angle. A 16 μm mylar film in front of the detector stopped elastically scattered deuterons while allowing the energetic protons into the detector. [N_{16O}] was determined with an uncertainty of 3% by comparing proton yields with the proton yield from a standard thermal Si$^{16}O_2$/Si film (Ref ^{16}O = 624.8 × 10^{15} at/cm^2). Typical NRA spectra are shown in Fig. 5. Note that in the spectrum obtained from the ^{17}O enriched sample, there is a significant interference in the $^{16}O(d,p_0)$ peak from $^{17}O(d,p_4)$, however there is no proton group from $^{17}O(d,p)$ that could interfere with the $^{16}O(d, p_1)$ peak.

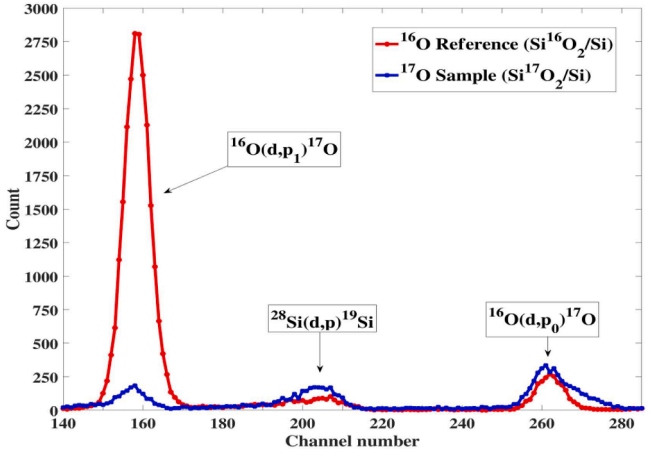

Fig. 5. Typical NRA spectra obtained from the ^{17}O enriched silica layer used for the cross section measurements, and a reference thin silica layer of natural isotopic composition.

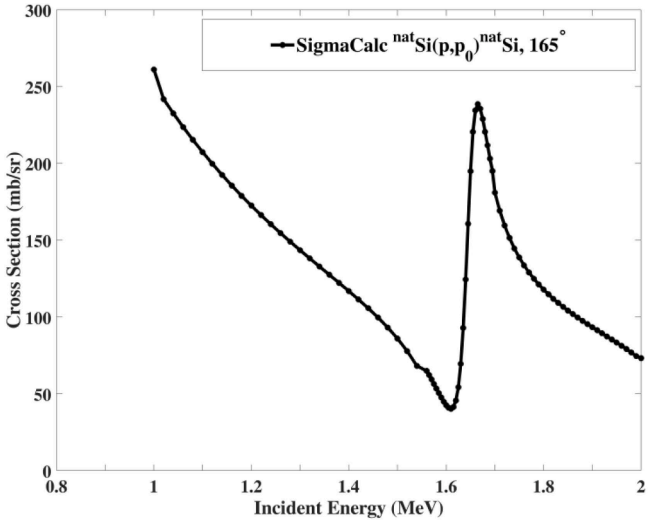

Fig. 6. ^{nat}Si(p,p) differential cross section curve.

2.4.4. Final target composition

A target of 107 ± 1 nm silica thickness was chosen for the cross section measurements. The total oxygen content from ellipsometry was 467 × 10^{15} at/cm^2, of which 18.2 × 10^{15} at/cm^2 were ^{18}O and 33.8 × 10^{15} at/cm^2 were ^{16}O. The areal density of ^{17}O [N_{17O}] in the sample was calculated to be 415 × 10^{15} at/cm^2 with an estimated uncertainty of about 5% mainly arising from counting statistics.

The film thickness deduced from RBS of this target, simulated supposing stoichiometry and a density of 2.21 g/cm^{-3}, is 105 nm. This is very close to the physical thickness measured by ellipsometry, indicating that the compound stopping power used in the SIMNRA calculation is reliable. Since the SIMNRA Ziegler/Biersack alpha particle stopping powers are scaled from proton stopping powers, this shows that it is reasonable to assume that the calculation of the average energy of the incident protons in the layer, for each of the incident energies chosen, is also reliable.

2.5. Determining the total oxygen peak area

2.5.1. Background suppression by ion channeling

For the ^{17}O target, which consists of a Si$^{17}O_2$ layer on a Si substrate, ion channeling is useful to suppress the background from the silicon substrate, allowing more accurate estimation of the area of the total oxygen peak ($Y_{\text{total O}}$). As shown in Fig. 6 the differential cross section of ^{nat}Si(p,p) around the energy 1670 keV is very high and rapidly varying. Under some conditions, this rendered determination of the oxygen peak area impossible, as may be seen in Fig. 7c. Here, channeling the incident beam in the substrate allowed the oxygen peak to be observed and its area estimated.

The sample was first aligned with an alpha particle beam, for which the critical channeling angles, larger than those of the proton beam, facilitate alignment. The alignment was refined with the proton beam. We noted no beam damage effects on the channeling spectra during the measurements, however it is to be noted that we are not very sensitive to damage effects since the amorphous oxide layer on the surface induced significant beam angular spread and minimum silicon yields were only about 30%, rather than the typical values of a few percent for fully crystalline structures.

2.5.2. Background subtraction

Our experiment requires extracting the area of the total oxygen peak ($Y_{\text{total O}}$), which is sitting on a large Si background that cannot be analytically modelled. In order to adjust a phenomenological background , we developed a user-friendly program which allows us to adjust a polynomial of arbitrary order, defined by the shape of the background curve only outside of the peak region, as shown in the regions between the two red cursors and the two blue cursors in Fig. 8. Because there is no a priori background shape, the goodness of the background is judged by the user. In all cases, the minimum possible polynomial order q was chosen, and uncertainties are estimated from fits based on extreme parameters for the definition of the fitting regions (outside the peak region) for which the background in the peak region is clearly erroneous, together with Monte Carlo uncertainty estimation using simulated data.

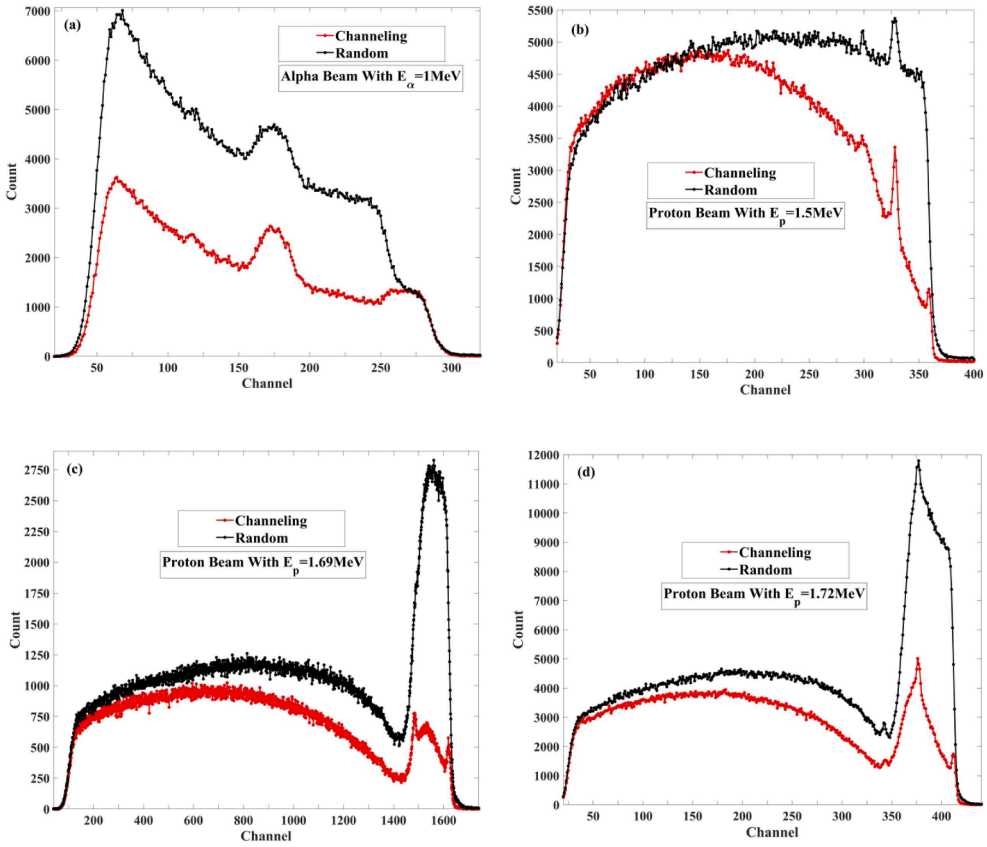

Fig. 7. The comparison between channelling and random peak at different with a) alpha beam with $E_\alpha = 1$ MeV, and proton beam with b) $E_p = 1.5$ MeV, c) $E_p = 1.69$ MeV and d) $E_p = 1.72$ MeV.

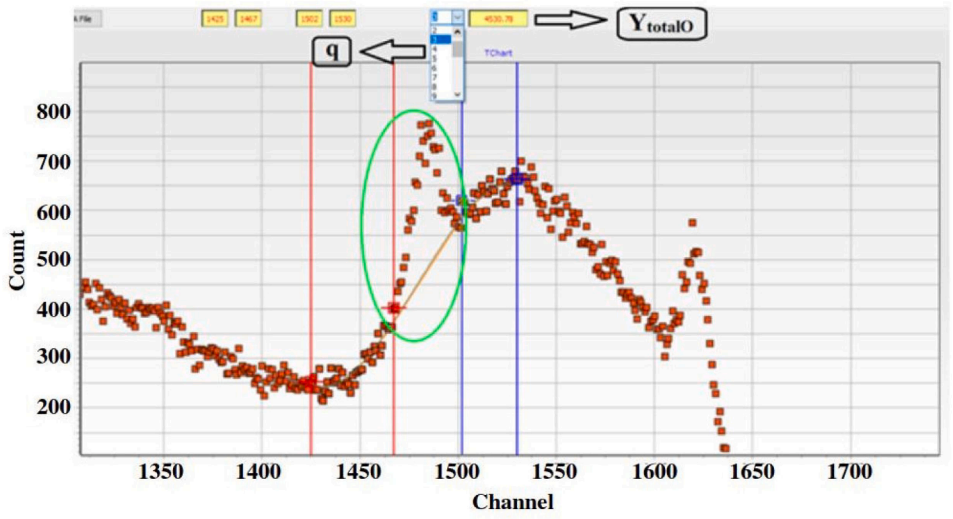

Fig. 8. Polynomial background determined for the spectrum of Fig. 7c, obtained with the proton beam aligned with the Si substrate ⟨100⟩ direction.

3. Results and discussion

The differential cross section of ^{17}O(p,p) was measured in the present work for $E_{p,lab} = 0.6$–2 MeV with 10 keV energy steps in most regions and 2 keV steps around the resonances (in Fig. 9).

The differential cross-sections for proton EBS on ^{17}O $\left(\frac{d\sigma}{d\Omega}\right)_{\theta,E(^{17}O(p,p))}$ at detection angle θ and incident proton energy E_p were obtained from Eq. (2):

$$\left(\frac{d\sigma}{d\Omega}\right)_{\theta,E(^{17}O(p,p))} = \frac{Y_{^{17}O,Ep}}{\Omega \times Q \times N_{^{17}O}} \tag{2}$$

with $Y_{^{17}O,Ep} = Y_{^{total}O,E_p} - Y_{^{18}O,Ep} - Y_{^{16}O,Ep}$; $Y_{^{16}O} = \Omega \times Q \times N_{^{16}O} \times \sigma_{^{16}O(p,p)}$, and $Y_{^{18}O} = \Omega \times Q \times N_{^{18}O} \times \sigma_{^{18}O}$ where $\Omega \times Q$, $N_{^{18}O}$ and $N_{^{16}O}$ were measured by ellipsometry as described in section 2.4.1 , p-NRA in section 2.4.2 and d-NRA in section 2.4.3, respectively. $^{total}O, Ep$ is defined in section 2-5.

$\sigma_{^{16}O(p,p)}$ was calculated by Sigmacalc at 165° at IBANDL with an en-

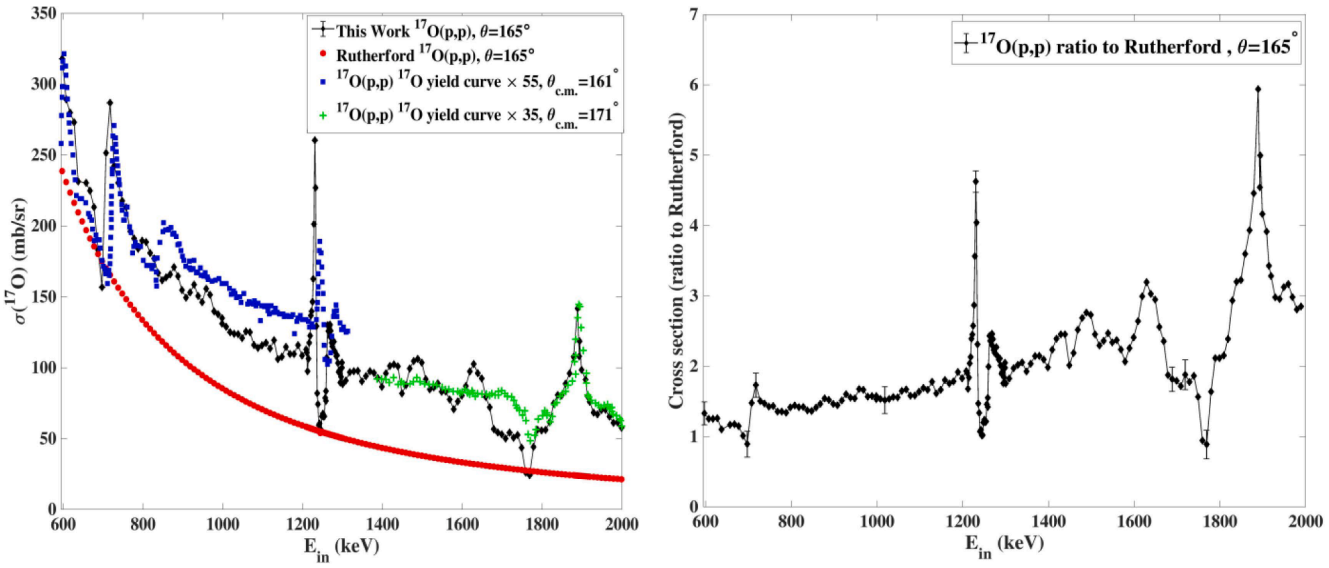

Fig. 9. a) Our measured proton elastic scattering cross-section, compared with scaled yield curves from Ref. [8,9]. b) The ratio to the Rutherford cross section of ^{17}O at 165° for E_p = 0.6–2 MeV in the laboratory system. The representative uncertainty bars in b) represent the statistical uncertainty.

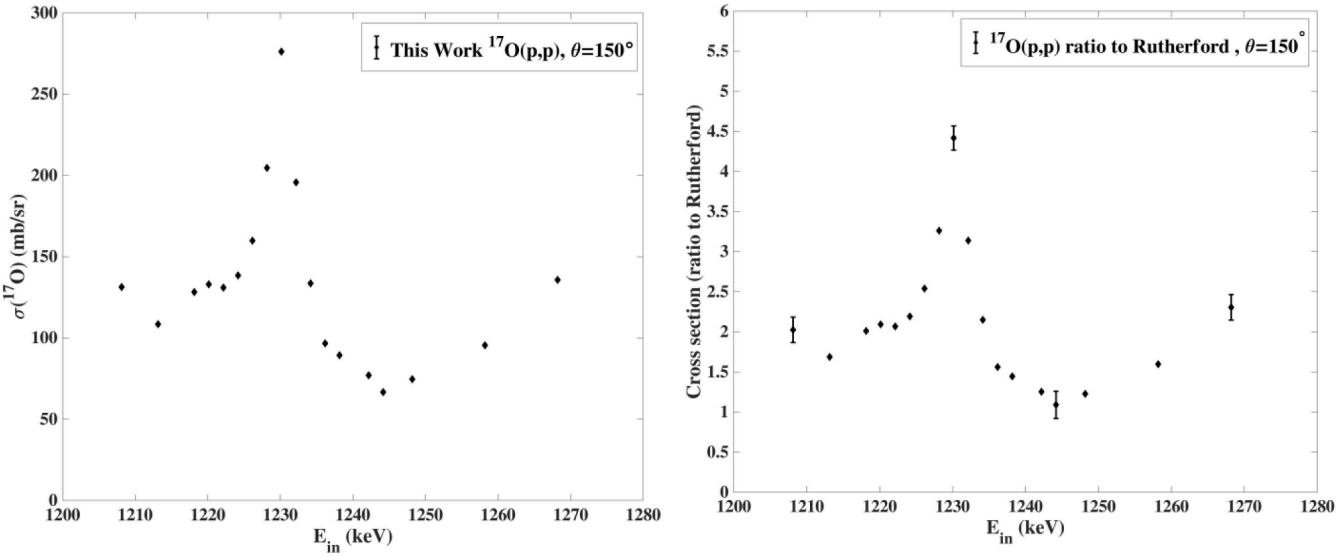

Fig. 10. a) Proton scattering cross-sections and b) the ratio to the Rutherford cross section of ^{17}O(p,p)^{17}O at 150° for E_p = 1.2–1.3 MeV in the laboratory system.

ergy step of 20 keV [4]. This calculation was interpolated by MATLAB to have the cross-sections of ^{16}O(p,p) for any arbitrary range of energy between 600 and 2000 keV. We could find no $\sigma_{^{18}O(p,p)}$ cross section data for 165° scattering angle, and so we used the closest existing data. $\sigma_{^{18}O(p,p)}$ was therefore derived from the only two measured data in IBANDL: Ref [11] in the energy range 590–1430 keV at 138.7° and Ref. [12] in the energy range 1.39–3.20 keV at 135°, also interpolated with MATLAB to give values for any required energy.

Finally, the proton scattering cross section for ^{17}O at 165° for E_p = 0.6–2 MeV in the laboratory system is presented in Fig. 9.a with the ratio to the Rutherford cross section being shown in Fig. 9.b. The energy values take into account the finite energy loss in the silica layer, which ranges from 5.8 keV at 600 keV incident energy, to 2.7 keV for 2 MeV incident protons. The systematic uncertainty is 14% (1σ) according to the standard error propagation formulas, including the uncertainty in identifying the contents of different isotopes of oxygen and the product $\Omega \times Q$. The uncertainty in the oxygen peak area determination, estimated by Monte Carlo treatment of the peak area extraction method (i.e. including variation in operator performance), is mostly between 4% and 6% and ranges from 3% to about 8% according to the peak intensity and the size and shape of the background to be estimated. The greatest uncertainty of 8% was obtained for the spectrum of Fig. 7(d).

There is an intense resonance with a maximum intensity at 1230 keV, of width about 4.5 keV after subtraction in quadrature of the target energy width of about 4 keV. We have also overlapped the scaled yield curves for $\theta_{cm} = 161°$ from [8] and$\theta_{cm} = 171°$ from [9]. The resonance energies are in good agreement with our measurement if the energy scale from [8] is scaled by 0.99. It is clear that the structure in the ^{18}O(p, p) cross section, unaccounted for when correcting the yield curves for the significant ^{18}O contamination in the gas used in [8] has led to marked differences between the measured yield curve and the cross section. We also note that the intensity of the resonance in the yield curve, compared to the continuous component, is smaller than that for the cross section, however the width of this resonance in the yield curve is very close to the width of 4.5 keV that we have observed in the cross section. This would give a depth resolution of around 50 nm in Si when

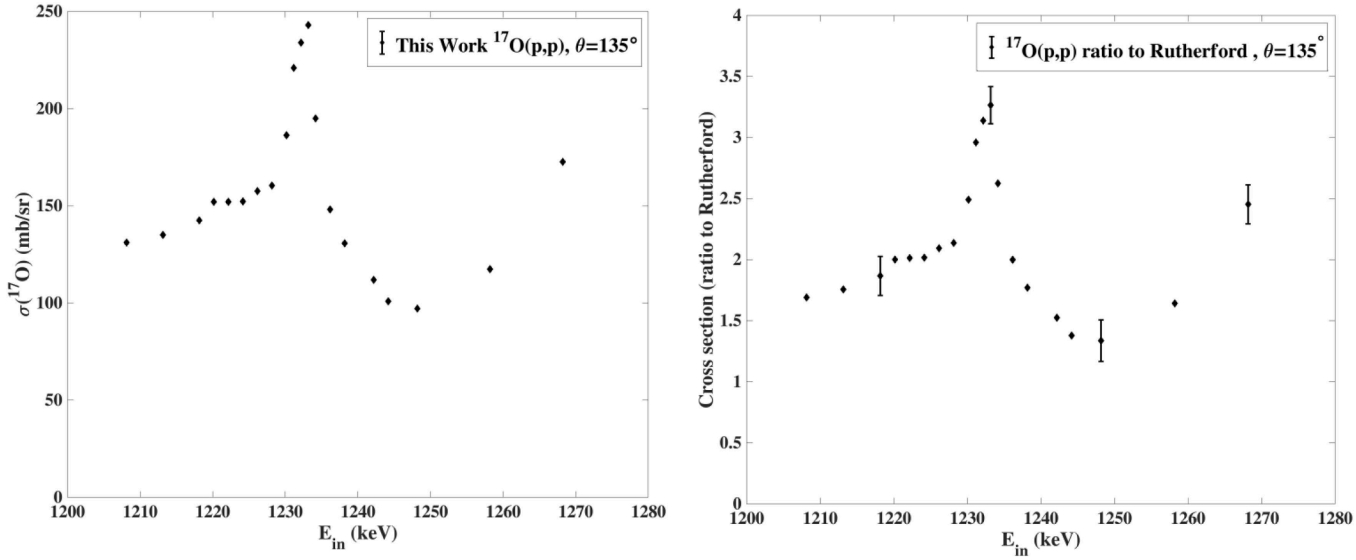

Fig. 11. a) Proton scattering cross-sections and b) the ratio to the Rutherford cross section of $^{17}O(p,p)^{17}O$ at 135° for E_p = 1.2–1.3 MeV in the laboratory system.

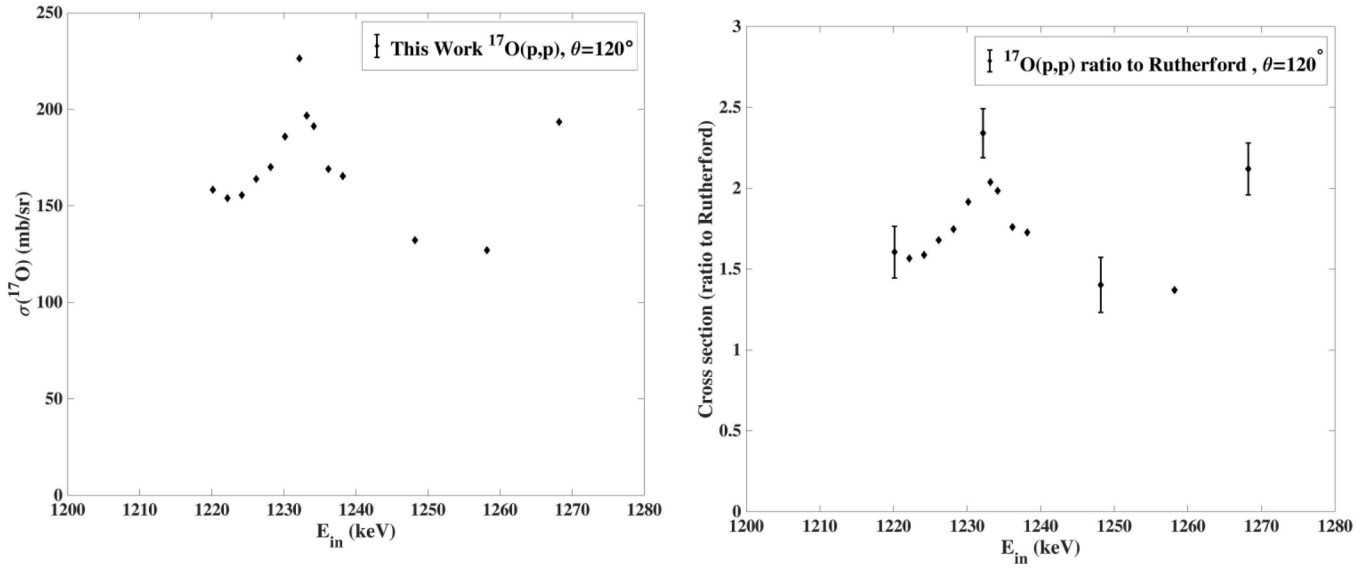

Fig. 12. a) Proton scattering cross-sections and b) the ratio to the Rutherford cross section of $^{17}O(p,p)^{17}O$ at 120° for E_p = 1.2–1.3 MeV in the laboratory system.

the beam energy is scanned around the resonance energy.

The yield curve from [9] was measured by the same group as that of [8], using a thin self-supporting target from which the protons scattered from ^{16}O and ^{18}O could be resolved from those scattered from ^{17}O. This yield curve, correctly scaled, should then represent the scattering cross section. There is a clear discrepancy between this scaled yield curve and our measurement below about 1.8 MeV. We cannot explain this discrepancy, however we note that the measured cross section is robust against possible systematic errors or bias in the delicate task of background subtraction, for which data reduction by two independent analysts yields results within the estimated random uncertainty margins. Further experimental work will be required to resolve the difference in shape between this yield curve and our cross section measurement.

In view of possible depth profiling applications we measured the cross section of $^{17}O(p,p)$ in the vicinity of this resonance at back scattering angles of 150, 135 and 120, shown in Figs. 10-12 respectively. From the comparison of the curves in Fig. 13, it is clear that the highest backscattering angle of 165° is to be preferred for ^{17}O depth profiling by EBS with this resonance.

The elastic scattering of protons on ^{17}O could be modelled with conventional phenomenological R-matrix theory [8,9], which could then provide a physical basis for the best estimates of cross sections for arbitrary energies and angles, however the R-matrix parameters would be determined with more reliability if cross sections at a number of angles contributed to their determination. Further measurements are planned in view of establishing a reliable R-matrix formulation for the absolute value of the cross section over a range of backscattering angles.

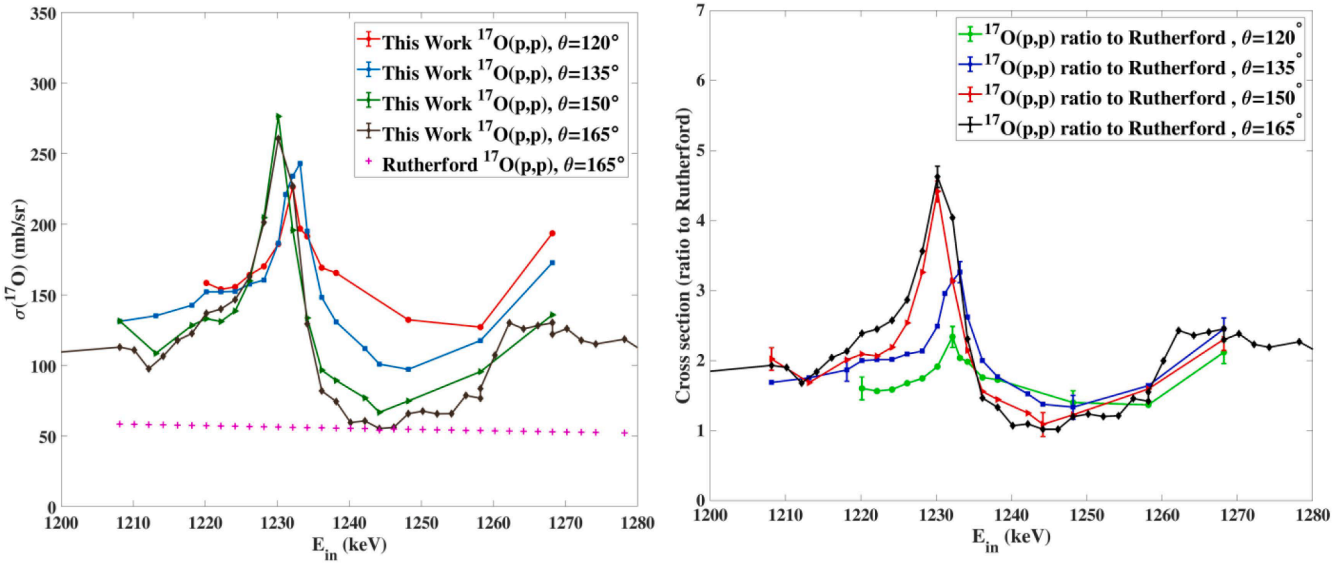

Fig. 13. Comparison of a) proton scattering cross-sections and b) the ratio to the Rutherford cross section of ^{17}O(p,p)^{17}O at different angles for E_p = 1.2–1.3 MeV in the laboratory system.

4. Conclusions

The elastic backscattering (EBS) cross section for protons on ^{17}O was measured for the first time. For energies in the range 600 keV to 2 MeV, and a laboratory scattering angle of 165°, the cross section consists of a smoothly varying component increasing from 1.2 times the Rutherford cross section at 600 keV up to about 3 times the Rutherford cross section at 2 MeV, on which are superposed a number of resonance structures. Amongst these, the intense EBS resonance of 4.5 keV width with a peak at 1230 keV has the most potential for concentration depth profiling of ^{17}O by beam energy scanning, especially at high backscattering angles, and could provide a depth resolution of about 50 nm in silicon.

Declaration of Competing Interest

The authors declare that they have no known competing financial interests or personal relationships that could have appeared to influence the work reported in this paper.

Acknowledgements

We are particularly indebted to S. Steydli (INSP) for assistance in mechanical and vacuum aspects, and H. Tancrez (INSP) for electronic and command-control systems development. M. Salimi would also like to express her deep appreciation of the strong support of M. Marangolo (Director of INSP) and N. Witkowski (Directrice of the Doctoral School) for her co-tutelle doctoral contract. M. Salimi gratefully acknowledges the contribution from CAMPUS FRANCE in support of her co-tutelle doctoral contract.

References

[1] A.R. Ramos, A. Paúl, L. Rijniers, M.F. da Silva, J.C. Soares, Measurement of (p, p) elastic differential cross-sections for carbon, nitrogen, oxygen, aluminium and silicon in the 500–2500 keV range at 140 and 178 laboratory scattering angles, Nucl. Instrum. Methods Phys. Res., Sect. B 190 (1-4) (2002) 95–99.

[2] Nastasi, M., J.W. Mayer, and Y. Wang, Ion beam analysis: fundamentals and applications. 2014: CRC Press.

[3] Gurbich, A. Differential Cross Sections for Elastic Scattering of Protons and Helions from Light Nuclei. in Lectures given at the Workshop on Nuclear Data for Science and Technology: Materials Analysis. 2003. http://users.ictp.it/~pub_off/lectures/lns022/Gurbich_2/Gurbich_2.ps.

[4] A.F. Gurbich, SigmaCalc recent development and present status of the evaluated cross-sections for IBA, Nucl. Instrum. Methods Phys. Res., Sect. B 371 (2016) 27–32.

[5] J. Demarche, G. Terwagne, Precise measurement of the differential cross section from the ^{16}O(α, α^{11}6O elastic reaction at 165° and 170° between 2.4 and 6.0 MeV, J. Appl. Phys. 100 (12) (2006), 124909.

[6] Battistig, G., et al., *A very narrow resonance in ^{18}O (p,α)^{15}N near 150 keV: Application to isotopic tracing. II. High resolution depth profiling of ^{18}O.* Nuclear Instruments and Methods in Physics Research Section B: Beam Interactions with Materials and Atoms, 1992. **66**(1-2): p. 1-10.

[7] Battistig, G., et al., *A very narrow resonance in ^{18}O(p,α)^{15}N near 150 keV: Application to isotopic tracing: I. Resonance width measurement.* Nuclear Instruments and Methods in Physics Research Section B: Beam Interactions with Materials and Atoms, 1991. **61**(4): p. 369-376.

[8] J.C. Sens, F. Rietsch, A. Pape, R. Armbruster, A spectroscopic study of 18F, Nucl. Phys. A 199 (2) (1973) 232–240.

[9] Sens, J., et al., *Search for simple configurations in F. 18 I. The ^{17}O(p,p)^{17}O reaction.* Physical Review C, 1977. **16**(6): p. 2129.

[10] K. Yagi, et al., Experiment on Elastic Scattering of Protons by ^{18}O, J. Phys. Soc. Jpn. 17 (4) (1962) 595–603.

[11] H. Kim, W. Milner, F. McGowan, Nuclear cross sections for charged-particle-induced reactions: N and O, Nuclear Data Sheets. Section A 3 (2) (1967) 123–127.

[12] D.L. Sellin, H.W. Newson, E.G. Bilpuch, High resolution investigation of resonances in ^{19}F, Ann. Phys. 51 (3) (1969) 461–475.

[13] M. Salimi, O. Kakuee, S.F. Masoudi, H. Rafi-kheiri, E. Briand, J.-J. Ganem, I. Vickridge, Determination and benchmarking of ^{27}Al(d, α) and ^{2}7Al(d, p) reaction cross sections for energies and angles relevant to NRA, Sci. Rep. 11 (1) (2021), https://doi.org/10.1038/s41598-021-97372-7.

[14] G. Amsel, D. Samuel, The mechanism of anodic oxidation, J. Phys. Chem. Solids 23 (12) (1962) 1707–1718.

[15] Deal, B.E. and C.R. Helms, *The physics and chemistry of SiO_2 and the Si-SiO_2 interface.* 2013: Springer Science & Business Media.

[16] N. Kitamura, K. Fukumi, J. Nishii, N. Ohno, Relationship between refractive index and density of synthetic silica glasses, J. Appl. Phys. 101 (12) (2007) 123533, https://doi.org/10.1063/1.2748861.

[17] S. Rigo, G. Barbottin, A. Vapaille, Instabilities in silicon devices, Silicon Passivation and Related Instabilities 1 (1986) 32.

[18] G. Amsel, D. Samuel, Microanalysis of the stable isotopes of oxygen by means of nuclear reactions, Anal. Chem. 39 (14) (1967) 1689–1698.